High-performance operation of single-mode terahertz quantum cascade lasers with metallic gratings

Cite as: Appl. Phys. Lett. **87**, 181101 (2005); https://doi.org/10.1063/1.2120901
Submitted: 26 April 2005 • Accepted: 06 September 2005 • Published Online: 24 October 2005

Lukas Mahler, Alessandro Tredicucci, Rüdeger Köhler, et al.

High-performance operation of single-mode terahertz quantum cascade lasers with metallic gratings

Lukas Mahler,[a] Alessandro Tredicucci, Rüdeger Köhler, and Fabio Beltram
NEST CNR-INFM and Scuola Normale Superiore, Piazza dei Cavalieri 7, 56126 Pisa, Italy

Harvey E. Beere, Edmund H. Linfield,[b] and David A. Ritchie
Cavendish Laboratory, University of Cambridge, Madingley Road, Cambridge CB3 0HE, United Kingdom

(Received 26 April 2005; accepted 6 September 2005; published online 24 October 2005)

A periodic array of thin slits opened on a metallic surface can act as a one-dimensional photonic crystal for the propagation of surface-plasmon waves. We have used such structure for the implementation of distributed feedback resonators in quantum cascade lasers emitting near 2.5 THz. Single-mode emission, stable at all injection currents and operating temperatures, was achieved both in pulsed and continuous wave. The devices exhibited output powers of several milliwatts with low threshold current densities of ~ 100 A/cm^2. © *2005 American Institute of Physics*.
[DOI: 10.1063/1.2120901]

Surface plasmons are electromagnetic waves existing at the interface between two materials, one with a positive and one (usually a metal) with a negative dielectric constant.[1] They are attracting considerable interest in view of their possible use in the implementation of photonic circuits and subwavelength optics.[2] They have also been employed in the construction of waveguides for quantum cascade (QC) lasers,[3] thanks to their intrinsic transverse-magnetic (TM) polarization, which ideally matches the selection rules of intersubband transitions. Surface-plasmon waveguides become particularly advantageous over traditional dielectric ones at long wavelengths, where they allow large optical confinement factors to be achieved in relatively thin active regions. In fact, they constitute a basic element of QC lasers operating in the 1–10 THz range;[4] these devices have rapidly reached a considerable level of maturity, with high output powers and operating temperatures reaching 164 K.[5–7]

Many laser applications require stable, repeatable single-mode emission at a precisely defined frequency. To this end distributed feedback (DFB) resonators[8] have long been used in semiconductor lasers including, more recently, midinfrared QC lasers.[9] The concept has now also been extended to terahertz frequency QC devices.[10] In that work mode selection was based on a complex-coupling scheme requiring a combination of wet chemical etching of the top contact layer and selective Ohmic-contact deposition. This technique, however, resulted in small grating coupling, thereby making long cavities necessary for the achievement of single-mode operation. This affected device performance, increasing driving currents and hindering continuous wave (cw) lasing. The issue becomes more and more critical at longer emission wavelengths as the DFB grating period has to be proportionally enlarged.

A different elegant way of realizing a one-dimensional photonic crystal for surface-plasmon modes was recently demonstrated.[11] A slit opened in the metallic layer acts as a barrier for wave propagation as no surface plasmon is supported. Part of the light is reflected back, part transmitted by tunneling across the slit, and part is scattered out of the interface mode. A periodic series of slits then acts as a DFB resonator, and, if the slits are much narrower than the wavelength, this can be accomplished with minimal scattering losses. Ideally, this type of metallic grating would be easily implemented in terahertz QC waveguides. However, the presence here of a top highly doped contact layer with negative dielectric constant ensures the existence of the surface-plasmon mode also in the slits. Although the radiation then does not propagate through tunneling, it still experiences much higher optical losses in the slits, owing to the higher penetration in the doped semiconductor, resulting in a DFB grating with a mainly imaginary coupling coefficient. Here we use this technique to demonstrate high-performance DFB devices operating near 2.5 THz, a frequency range particularly relevant for atmospheric monitoring of the OH radical.

The semiconductor sample used for this work is illustrated in Fig. 1. The active material (left panel) was designed for the GaAs/AlGaAs system and based on rather uniformly chirped superlattices, with no marked distinction between injection and lasing regions and an optical transition partly diagonal in real space. The calculated dipole matrix element is 10 nm for a transition energy around 10 meV. The ground state of each period is well separated from the injection barrier, in order to reduce the extent of possible leakage current paths that would decrease the injection efficiency. The structure was grown by solid-source molecular-beam epitaxy on a nominally undoped GaAs substrate, with a waveguide core formed by 110 repetitions of the above superlattice. Confinement of the emitted light was ensured by a buried highly doped GaAs layer with negative dielectric constant. Contrary to the conventional terahertz QC waveguide design,[4] however, the present layer features two different doping concentrations (the initial 530 nm is n doped to 2.6×10^{17} cm^{-3} and an additional 500 nm is doped to 2.7×10^{18} cm^{-3}). This allows the possibility of controlling separately the boundary conditions of the surface plasmons on the two sides of the buried doped layer, thereby giving a better compromise between optical losses and confinement factor.[12] The growth was concluded by a 200-nm-thick GaAs contact layer n

[a]Also at: Department of Physics, ETH Zurich, CH-8093 Zurich, Switzerland.
[b]Present address: School of Electronic and Electrical Engineering, University of Leeds, Leeds LS2 9JT, United Kingdom.

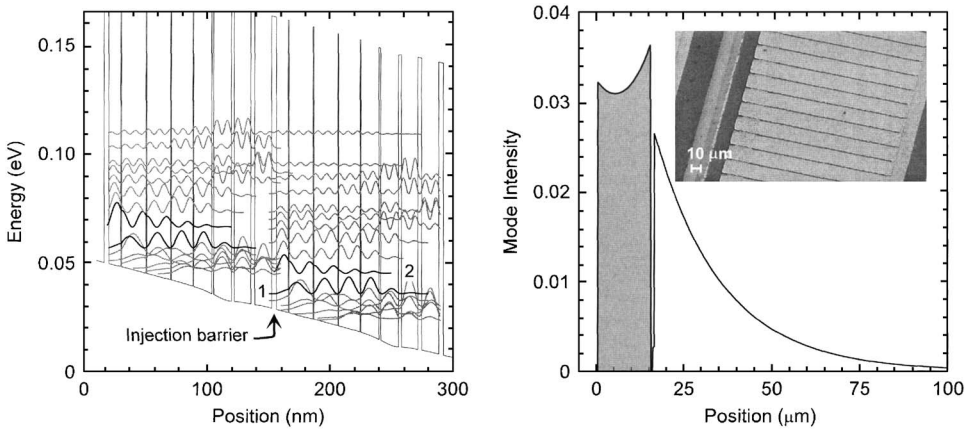

FIG. 1. Left panel: Conduction-band diagram for two periods of the 2.5 THz quantum cascade structure under an electric field of 1.6 kV/cm. The layer thicknesses in nanometers (from left to right, starting at the injection barrier) are **3.9**/9.6/**0.6**/19.9/**0.6**/19.4/**0.6**/17.5/**0.6**/14.7/**1.5**/14.4/**2.4**/13.4/**3.2**/13.7 where $Al_{0.15}Ga_{0.85}As$ barrier is in boldface and the last 10 nm of the 14.4 nm GaAs well is doped to $n=2.5\times10^{16}$ cm^{-3}. The moduli squared of the envelope functions of the relevant subbands are shown, with the optical transition taking place between levels 2 and 1. Right panel: Electric-field profile for the optical mode inside the device waveguide. The origin has been fixed at the top air-metal interface. The stack of 110 active periods is indicated by the shaded area. Inset: Scanning electron microscope picture of the top ridge metallization, showing the periodic array of thin slits. Also visible are the narrow-annealed Ohmic-contact stripes (appearing rougher) and one side of the laser ridge (at the left).

doped to 5×10^{18} cm^{-3}. Devices were processed into 240-μm-wide laser ridges by optical lithography, with Ohmic-contact deposition achieved using the procedure described in Ref. 13. The waveguide was completed by the evaporation of Cr/Au on top of the ridge to create the main surface-plasmon interface. This layer is kept either continuous for Fabry-Perot devices or patterned into a series of narrow slits with $\lambda/2$ period to create the DFB structure (see inset of Fig. 1). The fabrication of the latter was implemented by electron-beam lithography using a reduced metal thickness (100 nm instead of the usual 200 nm) to facilitate lift-off. The best compromise between grating strength and optical losses was found with approximately 2 μm wide slits (close to 10% of the period length). In this case the estimated coupling coefficient is of the order of 10 cm^{-1}. The vertical profile of the guided mode is plotted in Fig. 1 (right panel): a confinement factor of about 48% was obtained, with 10 cm^{-1} absorption losses. Individual lasers were defined by cleaving the ridges into stripes of various lengths. They were then soldered to copper bars with an In/Ag alloy, wire bonded, and mounted on the coldfinger of a continuous-flow liquid-helium cryostat. Spectra were recorded with a Fourier-transform infrared spectrometer in rapid scan mode at the maximum resolution of 0.125 cm^{-1}. Pulsed light-current (L-I) curves were obtained by collecting the output of one laser facet with $f/1$ off-axis parabolic optics and focusing it onto a pyroelectric detector, with the whole system contained within the cryostat head. Cw measurements were instead performed by mounting a $f/3.5$ Winston cone in front of the laser and using an external pyroelectric radiometer (estimated collection efficiency was $>33\%$).

Figure 2 shows the cw L-I characteristics for a conventional Fabry-Perot device. Excellent performance is achieved, with threshold current densities as low as 75 A/cm^2 observed at 10 K and a maximum operating temperature of 58 K. The measured output power is more than 6 mW with a slope efficiency of about 16 mW/A. The emission spectra (see inset) show multiple longitudinal modes with a spacing $\Delta\sim0.51$ cm^{-1}, which translate into a refractive index $n\sim3.9$. This differs from the computed effective index $n_{\text{eff}}=3.65$ of the waveguide mode, but the discrepancy is not unexpected in view of the rather large frequency dispersion $dn_{\text{eff}}/d\omega$. For the DFB fabrication we decided to use the calculated n_{eff} value, realizing gratings with periods varying from 16.2 to 16.6 μm. The left inset of Fig. 3 displays the pulsed emission spectra of three lasers with different surface-plasmon gratings. DFB operation is clearly demonstrated, with an emission frequency that depends on the grating period Λ according to a refractive index $n\sim3.56$, well within the parameter uncertainties of the theoretical value. The spectrum of the $\Lambda=16.2$ μm laser also shows a few Fabry-Perot modes, as the gain peak wavelength is now quite detuned from the DFB condition 2Λ. In fact, a longer device (2.5 mm) has to be used in this case to identify properly the DFB mode.

While these devices showed good DFB emission, even with very short cavity lengths of 1.5 mm (corresponding to less than 100 DFB periods), they were not reliably single mode over the whole range of operating conditions. At large

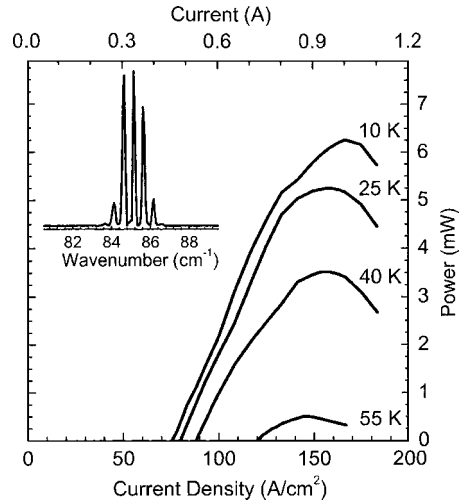

FIG. 2. Output power as function of drive current for a 2.5-mm-long 2.5 THz Fabry-Perot laser. The measurements are performed in continuous wave at various heat-sink temperatures. The maximum cw operating temperature is approximately 58 K. In the inset, a typical emission spectrum is displayed, showing lasing on multiple longitudinal modes.

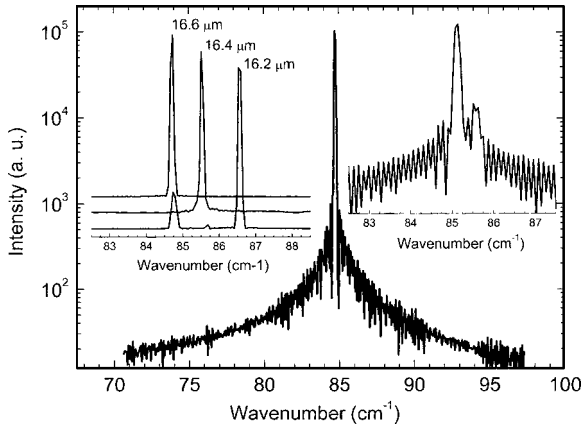

FIG. 3. Single-mode emission spectrum on a logarithmic scale of a 2.2-mm-long DFB laser with a 16.5 μm slit periodicity and narrow top metallization. Data were collected in pulsed mode at a 1% duty cycle and with a 0.92 A drive current, close to the maximum output power. In the left inset we plot in linear scale the spectra of three lasers with different DFB periods and a wide metallization. The upper two traces were collected close to threshold (about 350 mA), while the lowest trace was measured at a higher current in order to better show the DFB mode. The right inset shows a logarithmic plot of the spectrum at a higher current for the 16.4 μm laser of the left inset.

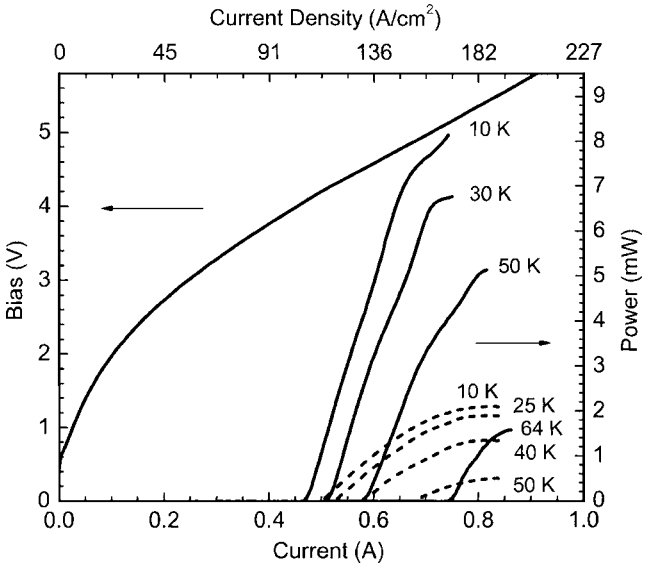

FIG. 4. Light-current characteristics of a 1.9-mm-long DFB QC laser. The solid lines refer to pulsed operation with 5% duty cycle and are collected using burst of 625 pulses 200 ns long at a repetition rate of 400 Hz; the dashed lines are obtained in cw using an external pyroelectric power meter (33% estimated collection efficiency) and correcting for the cryostat window transparency. The voltage measured as a function of drive current is also shown.

drive currents, a second mode often developed (right inset of Fig. 3), whose position seems at variance with another longitudinal mode. We attribute the second peak to a different transverse mode developing in the rather broad laser ridges. In order to prevent the formation of higher-order modes concentrated more towards the sides, we then fabricated lasers with a reduced metallization width, as exemplified in the inset of Fig. 1. The emission spectrum from one such laser with $\Lambda = 16.5$ μm is shown in a logarithmic scale in Fig. 3. This device is now stably single mode for all currents and temperatures with a high side-mode suppression ratio of more than 20 dB. The tuning of emission wavelength with temperature and current is within the resolution of the experimental apparatus.

The above-described fabrication technique yields efficient DFB gratings with excellent spectral performance. In order to realize a grating in which surface-plasmon propagation is interrupted in the slits, as described in the introduction, one possibility would be to etch away the doped semiconductor layer under the slits. A qualitatively similar result can also be achieved with a simpler procedure. Processing was carried out as described previously, but after the electron-beam lithography the lift-off step was avoided. As a consequence, a layer of resist approximately 400 nm thick is left in the slits and everything is then covered by metal. The laser mode has a strong penetration in the resist, thus considerably reducing the confinement factor (approximately by a factor of 2), increasing losses, and also introducing a spatial mismatch with the unperturbed mode that gives rise to the increased reflectance at each slit. DFB lasers produced in this way displayed the best performance in terms of output power and temperature dependence. This is likely to be a result of low radiation scattering out of a fully metallized ridge. Figure 4 shows the *L-I* characteristics of one such DFB laser. The device, which is stably single mode under all investigated conditions, emits more than 8 mW peak power per facet in pulsed at 10 K, with a threshold current density of about 100 A/cm^2 and a maximum operating temperature of 70 K. In cw the measured power was about a factor of 3 less even at low temperature. This might partially result from the different collection efficiencies of the two setups. The maximum operating temperature in this case was 55 K. The voltage-current curve is also plotted in Fig. 4, showing a typical diodelike behavior with very good injection efficiency.

This work was supported in part by the European Commission through the IST project "Teranova" and the Marie Curie RTN "Poise," and by Physical Sciences Inc. The authors are thankful to C. Mauro and R. Green for their assistance.

[1] See, for instance, P. Yeh, *Optical Waves in Layered Media* (Wiley, New York, 1988).
[2] W. L. Barnes, A. Dereux, and T. W. Ebbesen, Nature (London) **424**, 824 (2003).
[3] C. Sirtori, C. Gmachl, F. Capasso, J. Faist, D. L. Sivco, A. L. Hutchinson, and A. Y. Cho, Opt. Lett. **23**, 1366 (1998).
[4] R. Köhler, A. Tredicucci, F. Beltram, H. E. Beere, E. H. Linfield, A. G. Davies, D. A. Ritchie, R. C. Iotti, and F. Rossi, Nature (London) **417**, 156 (2002).
[5] B. S. Williams, S. Kumar, Q. Hu, and J. L. Reno, Opt. Express 13, 3331 (2005).
[6] S. Barbieri, J. Alton, H. E. Beere, J. Fowler, E. H. Linfield, and D. A. Ritchie, Appl. Phys. Lett. **85**, 1674 (2004).
[7] L. Ajili, G. Scalari, J. Faist, H. E. Beere, E. H. Linfield, D. A. Ritchie, and A. G. Davies, Appl. Phys. Lett. **85**, 3986 (2004).
[8] H. Kogelnik and C. V. Shank, J. Appl. Phys. **43**, 2327 (1972).
[9] J. Faist, C. Gmachl, F. Capasso, C. Sirtori, D. L. Sivco, J. N. Baillargeon, A. L. Hutchinson, and A. Y. Cho, Appl. Phys. Lett. **70**, 2670 (1997).
[10] L. Mahler, R. Köhler, A. Tredicucci, F. Beltram, H. E. Beere, E. H. Linfield, D. A. Ritchie, and A. G. Davies, Appl. Phys. Lett. **84**, 5446 (2004).
[11] J. C. Weeber, Y. Lacroute, A. Dereux, E. Devaux, T. Ebbesen, C. Girard, M. U. González, and A. L. Baudrion, Phys. Rev. B **70**, 235406 (2004).
[12] D. Indjin, Z. Ikonić, P. Harrison, and R. W. Kelsall, J. Appl. Phys. **94**, 3249 (2003).
[13] R. Köhler, A. Tredicucci, F. Beltram, H. E. Beere, E. H. Linfield, A. G. Davies, D. A. Ritchie, S. Dhillon, and C. Sirtori, Appl. Phys. Lett. **82**, 1518 (2003).